Simultaneous diffusion MRI and PET imaging of breast cancer patients

Eric Edward Sigmund[1], Sungheon Kim[1], Christian Geppert[2], Linda Moy[3], David Faul[2], Christopher Glielmi[2], Kimberly Jackson[3], Kamil Bani-baker[3], and Amy Melsaether[3]

[1]*Radiology, NYU Langone Medical Center, Bernard and Irene Schwartz Center for Biomedical Imaging, New York, NY, United States,* [2]*Siemens Medical Systems, New York, NY, United States,* [3]*Radiology, NYU Langone Medical Center, New York, NY, United States*

Target Audience: Physicists and radiologists interested in quantitative oncological imaging on the whole-body simultaneous MR/PET platform.

Purpose: Effective diagnosis and treatment of breast cancer requires understanding multifactorial complexity [1]. Magnetic resonance (MR) diffusion-weighted imaging (DWI) and fluorodeoxyglucose (FDG) positron emission tomography (PET) sense different components of tumor cell proliferation, providing complementary sensitivities [2]. Cancer cell proliferation reduces the extracellular space and thus the apparent diffusion coefficient (ADC) [3-6]. FDG-PET measures consumption of deoxyglucose feeding the proliferation process. Studies have found moderate inverse correlation between ADC and FDG-PET standard uptake value (SUV) [7,8], indicating a connection between tumor cell abundance and glucose demand requiring further elucidation. Since the intravoxel incoherent motion (IVIM) diffusion model [9-12] has been shown to provide valuable biomarkers of vascularity and cellularity in breast cancer, we collected simultaneous IVIM and FDG-PET in 3 breast cancer patients.

Methods: A whole-body integrated 3 T MR/PET scanner (Siemens Biograph mMR) was used to simultaneously acquire MRI and PET images of the breast in the prone position with a dedicated 4-channel breast coil (Noras, Würzburg, Germany), following their scheduled PET/CT and without additional FDG injection. The coil was imaged in a dual energy CT scanner to generate a μ-map for attenuation correction of the PET data. A flexible body-matrix array coil was placed on the patient's back but only activated for the attenuation-correction (AC) coronal 3D Dixon VIBE scan. Contrast-enhanced MRI was acquired with a prototype radial VIBE sequence [13]. Diffusion-weighted images were collected with a twice-refocused spin echo sequence with echo planar readout with SPAIR and extra fat suppression, using b-values of b= 0,30,70,100,150,200,300,400,500,800 s/mm^2. PET events were simultaneously accumulated for 15 minutes and images were reconstructed on the vendor platform incorporating μ-maps from both the RF coil and the MR AC scan. DWI analysis was performed within Igor Pro (Wavemetrics, Inc.). Monoexpential decay analysis was performed using all b-values to generate apparent diffusion coefficient (ADC) maps. Regions of interest were drawn enclosing various lesions, fibroglandular tissue (FGT), or other entities on DWI with guidance both from the ADC map (where lower values suggest malignant tissue) the post-contrast image (where hyperintensity indicates high blood volume and vascular permeability), and the PET images. Integrated signal intensities were fit with a segmented algorithm to the two-compartment IVIM model to extract tissue diffusivity D_t, perfusion fraction f_p, and pseudodiffusivity D_p. ROIs were drawn on the PET image in the lesions using Siemens SyngoVia software to extract mean, maximum, and minimum SUV.

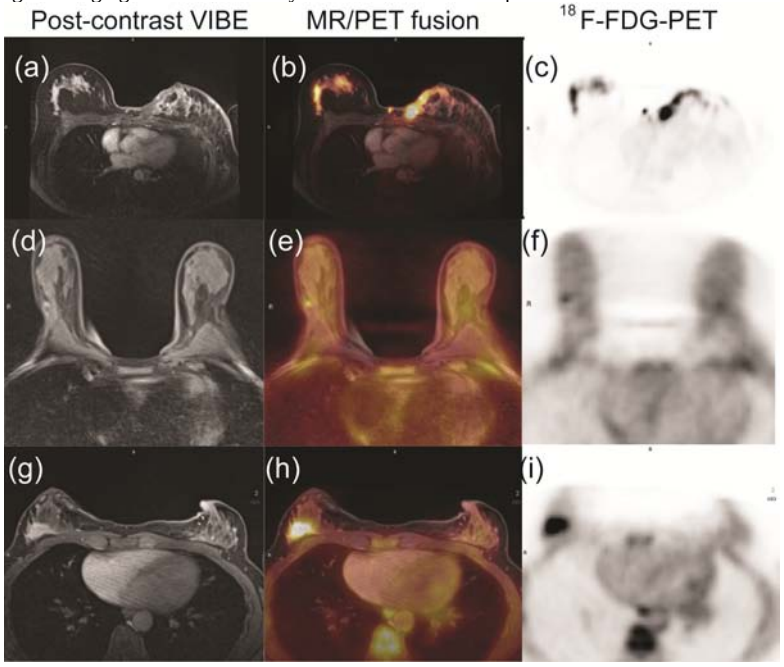

Figure 1: Simultaneous MR/PET imaging of patients with local breast cancer. (a)-(c) complex multifocal disease; (d)-(f): small lesion; (g)-(i) large malignant lesion. Gray/colorscales are individually adjusted for conspicuity.

Results: Figure 1 shows images from three patients with breast cancer (multifocal cancer in a patient with metastatic (stage 4) disease, an 8 mm IDC (T1b) and a 3 cm mixed IDC/ILC(T1c)), including post-contrast VIBE, PET, and MR/PET fusion. Figure 2a shows example IVIM ROI signal decays from the patient in Figure 1g-i. Figure 2b-d shows a representation of the values derived from quantitative IVIM and PET imaging in each cancer or other entity. Malignant lesions generally showed higher f_p (10.1 vs. 3.8%), lower D_t (1.35 vs. 1.96 μm^2/ms), and higher mean SUV (3.8 vs. 0.8 mBq/ml) than FGT; however, certain entities break this pattern. Cellulitis shows very high FDG activity, very restricted diffusion, and moderate vascularity as part of the inflammatory process; in this case D_t and SUV might indicate malignancy but f_p less aggressiveness. Conversely, the treated cancerous lesion's minimal activity and nearly unrestricted diffusion indicates cytotoxic effect but the lesion remains moderately vascular, distinguishing it from FGT.

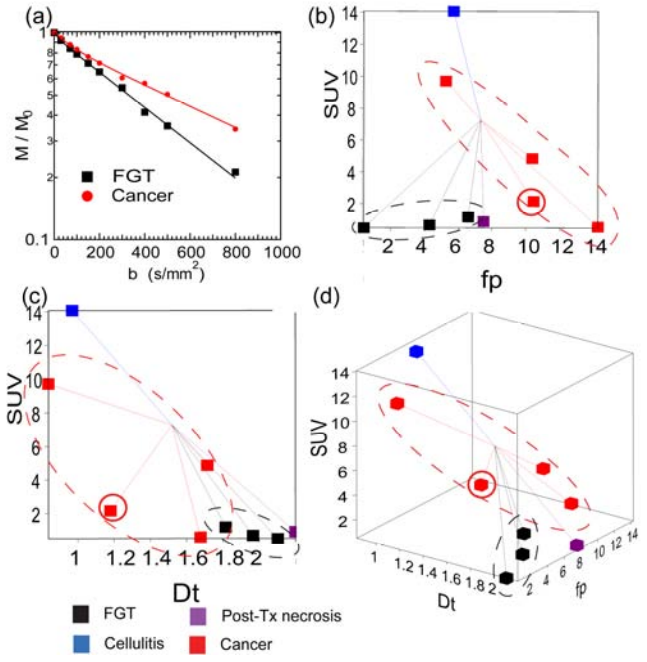

Figure 2: (a) IVIM fits from patient shown in Fig. 1g-i; result indicated by red circle in (b-d): MR/PET parameters (D_t (μm^2/ms), f_p(%), mean SUV (MBq/ml)) in breast lesions and FGT. Trends of malignancy (lower D_t, higher f_p, higher SUV) are observed in lesions compared to other entities, but multiparametric data provides unique lesion characterization.

Discussion: This preliminary study shows the feasibility of collecting simultaneous IVIM-MRI and PET biomarkers in breast MR/PET examinations with a dedicated breast coil. Both modalities classify malignancies according to expected trends, but their combination show potential subtle specificity advantages not observed in either modality alone. Larger scale studies are warranted to more carefully determine correlations between diffusion MR and glucose consumption, and their prognostic potential for predicting treatment response.

References: 1.Bell LK, Nmr Biomed 2011;24(6):612-635. 2. Kwee TC, J Nucl Med 2010;51(10):1549-1558. 3. Thoeny HC, JMRI 2010;32(1):2-16. 4.Sinha S, JMRI 2002;15(6):693-704. 5. Partridge SC, JMRI 2010;31(3):562-570. 6. Chen X, Bmc Cancer 2010;10:693. 7. Nakajo M, Eur J Nucl Med Mol Imag 2010;37(11):2011-2020. 8. Park SH, Eur Radiol 2012;22(1):18-25. 9. Lebihan D, Radiology 1988;168(2):497-505. 10. Kim S, Nmr Biomed 2012;25(5):787-794. 11. Sigmund EE, MRM 2011;65(5):1437-1447. 12. Lemke A, Invest. Radiol. 2009;44(12):769-775. 13. Chandarana H, Invest Radiol. 2011;46(10):648-53.